

A deep wide-field optical survey in the young open cluster Collinder 359 ★ ★★

N. Lodieu^{1,2} ★★, J. Bouvier³, D. J. James^{3,4}, W. J. de Wit³, F. Palla⁵, M. J. McCaughrean^{2,6}, and J.-C. Cuillandre⁷

¹ Department of Physics & Astronomy, University of Leicester, University Road, Leicester LE1 7RH, UK
e-mail: nl41@star.le.ac.uk

² Astrophysikalisches Institut Potsdam, An der Sternwarte 16, 14482 Potsdam, Germany

³ Laboratoire d'Astrophysique, Observatoire de Grenoble, BP 53, 38041 Grenoble Cédex 9, France
e-mail: Jerome.Bouvier@obs.ujf-grenoble.fr, Willem-Jan.DeWit@obs.ujf-grenoble.fr

⁴ Physics and Astronomy Department, Vanderbilt University, 1807 Station B, Nashville, TN 37235, USA
e-mail: david.j.james@vanderbilt.edu

⁵ INAF, Osservatorio Astrofisico di Arcetri, Largo E. Fermi 5, 50125 Florence, Italy
e-mail: palla@arcetri.astro.it

⁶ University of Exeter, School of Physics, Stocker Road, Exeter EX4 4QL, UK
e-mail: mjm@aip.de, mjm@astro.ex.ac.uk

⁷ Canada-France-Hawaii Telescope Corp., Kamuela, HI 96743, USA
e-mail: jcc@cft.hawaii.edu

Received February 5, 2008 /Accepted

Abstract. We present the first deep, optical, wide-field imaging survey of the young open cluster Collinder 359, complemented by near-infrared follow-up observations. This study is part of a large programme aimed at examining the dependence of the mass function on environment and time. We have surveyed 1.6 square degrees in the cluster, in the I and z filters, with the CFH12K camera on the Canada-France-Hawaii 3.6-m telescope down to completeness and detection limits in both filters of 22.0 and 24.0 mag, respectively. Based on their location in the optical ($I - z, I$) colour-magnitude diagram, we have extracted new cluster member candidates in Collinder 359 spanning $1.3\text{--}0.03 M_{\odot}$, assuming an age of 60 Myr and a distance of 450 pc for the cluster. We have used the 2MASS database as well as our own near-infrared photometry to examine the membership status of the optically-selected cluster candidates. Comparison of the location of the most massive members in Collinder 359 in a $(B - V, V)$ diagram with theoretical isochrones suggests that Collinder 359 is older than α Per but younger than the Pleiades. We discuss the possible relationship between Collinder 359 and IC 4665 as both clusters harbour similar parameters, including proper motion, distance, and age.

Key words. Open clusters and associations: individual: Collinder 359 — Stars: low-mass, brown dwarfs — Techniques: photometric

1. Introduction

The number of known brown dwarfs (hereafter BDs) has increased dramatically over the past few years, in the field (Kirkpatrick et al. 1999, 2000; Burgasser et al. 2002; Cruz et al. 2003), as companions to low-mass stars

Send offprint requests to: N. Lodieu

* Based on observations obtained at Canada-France-Hawaii Telescope

** Table 4 is only available in electronic form at the CDS via anonymous ftp to cdsarc.u-strasbg.fr (130.79.128.5)

*** Visiting Astronomer, German-Spanish Astronomical Centre, Calar Alto, operated by the Max-Planck-Institute for Astronomy, Heidelberg, jointly with the Spanish National Commission for Astronomy.

(Burgasser et al. 2003; Gizis et al. 2003; Close et al. 2003; Bouy et al. 2003), in star-forming regions (Lucas & Roche 2000; Briceño et al. 2002; Luhman et al. 2003), and in open clusters (Bouvier et al. 1998; Zapatero Osorio et al. 2000; Barrado y Navascués et al. 2001a; Barrado y Navascués et al. 2002; Oliveira et al. 2003, and references therein). Since the discovery of the first BDs in the Pleiades (Rebolo et al. 1995, 1996), numerous open clusters have been targeted in the optical and in the near-infrared to uncover their low-mass and substellar populations, including the Pleiades (Bouvier et al. 1998; Tej et al. 2002; Dobbie et al. 2002a; Moraux et al. 2003), α Per (Stauffer et al. 1999; Barrado y Navascués et al. 2002), M 35 (Barrado y Navascués et al. 2001a), IC 2391 (Barrado y Navascués et al. 2001b), and NGC 2547 (Oliveira et al. 2003).

The knowledge of the Initial Mass Function (hereafter IMF) is of prime importance in understanding the formation of stars. The IMF is fairly well constrained down to about

$0.5 M_{\odot}$ and well approximated by a three segment power law with $\alpha = 2.7$ for stars more massive than $1 M_{\odot}$, $\alpha = 2.2$ from 0.5 to $1.0 M_{\odot}$, and $\alpha = 0.7$ – 1.85 in the 0.08 – $0.5 M_{\odot}$ mass range with a best estimate of 1.3 (Kroupa 2002), when expressed as the mass spectrum. However, the mass spectrum remains somewhat uncertain in the low-mass and substellar regimes. Most studies conducted in Pleiades-like open clusters suggest a power law index α in the range 0.5 – 1.0 across the hydrogen-burning limit (Martín et al. 1998; Bouvier et al. 1998; Tej et al. 2002; Dobbie et al. 2002a; Moraux et al. 2003; Barrado y Navascués et al. 2001a; Barrado y Navascués et al. 2002). A comparable result is obtained for the mass function in the solar neighbourhood (Kroupa et al. 1993; Reid et al. 1999).

Several theories have recently emerged to explain the formation of BDs. First, the picture of the turbulent fragmentation of molecular clouds can be extended to lower masses (Klessen 2001; Padoan & Nordlund 2002). Second, Whitworth & Zinnecker (2004) proposed that BDs could result from the erosion of pre-stellar cores in OB associations. Third, gravitational instabilities of self gravitating protostellar disks might also be responsible for the formation of BDs (Watkins et al. 1998a,b; Lin et al. 1998; Boss 2000). Moreover, BDs could stop accreting gas from the molecular cloud due to an early ejection from a multiple system (Reipurth & Clarke 2001; Bate et al. 2002; Delgado-Donate et al. 2003; Sterzik & Durisen 2003). Finally, as BDs straddle the realms of stars and planets, they might form within a circumstellar disk in a similar manner to giant planets (Papaloizou & Terquem 2001; Armitage & Bonnell 2002).

Observational evidence for disks around young BDs has been reported in several star-forming regions in the near-infrared (Muench et al. 2002; Wilking et al. 1999; Luhman 1999; Oliveira et al. 2002), in the L' -band at $3.8 \mu\text{m}$ (Liu et al. 2003; Jayawardhana et al. 2003), in the mid-infrared (Natta et al. 2002; Testi et al. 2002; Apai et al. 2002), and at millimetre wavelengths (Klein et al. 2003). These results suggest a common formation mechanism for stars and BDs. The recent lack of substellar objects in Taurus compared to the Trapezium Cluster and IC 348 (Briceño et al. 2002; Luhman et al. 2003) and the distinctive binary properties of field BDs (Reid et al. 2001; Burgasser et al. 2003; Gizis et al. 2003; Close et al. 2003; Bouy et al. 2003) hint that stars and BDs may represent two independent populations (Kroupa et al. 2003). Additional studies of nearby field BDs and young BDs in open clusters are necessary to pin down on the formation mechanism(s) of substellar objects.

We have initiated a large Canada-France-Hawaii Telescope Key Programme (CFHTKP) surveying 80 square degrees in star-forming regions (≤ 3 Myr), pre-main-sequence clusters (10–50 Myr), and in the Hyades (700 Myr) in I and z filters with the CFH12K wide-field camera. The goal of our project is to investigate in an homogeneous manner the dependence of the IMF with time and environment as well as the distribution of stars and BDs in clusters to provide clues on their formation. Our detection and completeness limits are $(I, z) \sim 24$ and 22 mag in both passbands, respectively. In this paper, we present the results of a 1.6 square degree (5 CFH12K fields-

of-view) survey complemented by near-infrared photometry in one young open cluster, Collinder 359 (= Melotte 186).

Collinder 359 is a young open cluster located in the Ophiuchus constellation around the B5 supergiant 67 Oph (HD 164353). The cluster was first mentioned by Melotte (1915) as a “large scattered group of bright stars” and its presence confirmed later by Collinder (1931). A handful of cluster members are known (Collinder 1931; Van’t-Veer 1980; Rucinski 1987). It lies between 200 pc (Lyngå 1987) and 650 pc (Kharchenko 2004; personal communication) with a mean value of 435 pc from the HIPPARCOS parallax measurement (Perryman et al. 1997). The age of Collinder 359 is estimated to be about 30 Myr (Wielen 1971; Abt & Cardona 1983).

This paper is structured as follows: A literature review of our current knowledge of Collinder 359 is presented in §2 including a discussion regarding its proper motion, distance and age. In §3, we briefly introduce the framework of the CFHTKP. The 1.6 square degree, wide-field optical survey of Collinder 359 is detailed in §4. A description of the candidate cluster member selection process, using an optical ($I - z$, I) colour-magnitude diagram, is given in §5. Finally, in §6, we present details of a near-infrared follow-up survey of optically-selected candidate members in Collinder 359.

2. The open cluster Collinder 359

Collinder 359 was selected as a 30 Myr pre-main-sequence open cluster at a distance of 250 pc within the framework of our CFHTKP using data obtained from the WEBDA open clusters database¹. The equatorial and Galactic coordinates (J2000) of the cluster centre are ($18^{\text{h}}01^{\text{m}}, +02^{\circ}54'$) and ($29.7, +12.5$), respectively. Very little is known about Collinder 359 and no deep optical survey has been conducted in the cluster to date. We give below a brief overview of the current knowledge on the cluster.

Collinder 359 was first seen on the Franklin-Adams Charts Plates by Melotte (1915) and listed in his large catalogue of globular and open clusters. Melotte (1915) classified Collinder 359 as a “coarse cluster” and described it as “a large scattered group of bright stars around 67 Ophiuchi, covering an area of about 6 square degrees”. In his catalogue of open clusters, Collinder (1931) described it as “a group of about 15 stars with no appreciable concentration on the sky and no well-defined outline” and added that “cluster stars appear brighter than the surrounding stars but no bright stars stand out from the others”. The diameter of the cluster was estimated to 240 arcmin and dimensions of $5^{\circ} \times 3^{\circ}$ were also mentioned.

Collinder (1931) listed 13 cluster members and provided coordinates, photometry, spectral types, and proper motion information when available (Table 1; filled circles in Fig. 4). Additional photometry was compiled by Blanco et al. (1968). Isochrone fitting to five early-B stars yielded photometric parallax of 0.0048 ($d = 209$ pc) while the fainter B8–A2 stars gave a mean parallax of 0.0035 ($d = 286$ pc). However, the membership of these objects is not well established and trig-

¹ The WEBDA database, maintained by J.-C. Mermillod, is to be found at <http://obswww.unige.ch/webda/>

Table 1. This table lists the 13 bright stars within Collinder 359 as listed by Collinder (1931). Column 1 lists the running number of the member, column 2 gives the Henry Draper Catalogue number, columns 3 and 4 list the right ascension and the declination (in J2000), column 5 lists the spectral types (Collinder 1931), columns 6, 7, and 8 lists the V magnitude and the $B - V$ and $U - B$ from Blanco et al. (1968), columns 9 and 10 list the $V - R$ and $R - I$, columns 11 and 12 list the proper motion (arcsec per year) of the object according to the SAO catalogue (1966), column 13 gives the HIPPARCOS parallax π (Perryman et al. 1997). The membership of the object is given on the last column according to the discussion between Rucinski (1980) and Van't-Veer (1980).

N°	HD	RA	Dec	SpT	V	$B - V$	$U - B$	$V - R$	$R - I$	μ_α	μ_δ	π	M?
1	161868	17 47 53.5	02 42 26	A0	3.74	+0.03	+0.14	0.01	0.00	-0.0240	-0.074	34.42±0.99	NM
2	164353	17 58 08.3	02 55 57	B5 Ib	3.96	+0.04	-0.63	0.06	0.03	-0.0015	-0.010	2.30±0.77	M
3	164577	18 01 45.2	01 18 18	A2	4.43	+0.04	+0.05	0.04	0.01	+0.0090	-0.012	12.31±0.83	NM
4	164284	18 00 15.8	04 22 07	B3	4.70	-0.04	-0.86	0.10	0.08	+0.0000	-0.013	4.82±0.78	NM
5	166233	18 09 33.8	03 59 35	F2	5.72	+0.37	+0.02	0.22	0.21	+0.0360	-0.007	19.62±1.22	NM
6	165174	18 04 37.3	01 55 08	B3	6.14	-0.01	-0.98	0.03	0.03	-0.0045	-0.003	-0.76±0.89	NM
7	168797	18 21 28.4	05 26 08	B5	6.16	-0.02	-0.64	0.00	0.01	+0.0105	-0.004	0.97±0.83	NM
8	164432	18 00 52.8	06 16 05	B3	6.35	-0.08	-0.77	-0.01	-0.01	+0.0015	-0.003	2.17±0.87	M
9	163346	17 55 37.5	02 04 29	A3	6.78	+0.56	+0.36	0.37	0.40	-0.0030	+0.007	5.07±0.87	NM
10	164097	17 59 29.5	02 20 37	A2	8.54	+0.17	+0.15	0.12	0.15	-0.0060	+0.003	—	M
11	164283	17 57 42.4	05 32 37	A0	9.10	+0.26	+0.19	0.16	0.21	+0.0075	-0.014	4.11±1.27	M
12	164352	18 00 41.7	03 08 57	B8	9.33	-0.01	-0.39	0.02	0.06	-0.0015	-0.002	—	M
13	164096	17 59 34.6	02 30 16	A2	9.70	+0.20	+0.17	0.13	0.20	-0.0105	-0.006	—	M

gered a discussion based on a new CCD photometry between Rucinski (1980), Van't-Veer (1980), and Rucinski (1987). Later, Baumgardt et al. (2000) combined photometry, radial velocities, and parallaxes to reject some objects originally proposed as members.

2.1. The cluster proper motion

Collinder 359 has a small proper motion according to the original study by Collinder (1931) and the more recent measurement from the astrometric satellite HIPPARCOS. The proper motion of the cluster is comparable to the motion of 67 Oph, its most massive member, and was estimated as 0.42 ± 0.47 mas/yr in right ascension and -7.86 ± 0.35 mas/yr in declination (Baumgardt et al. 2000). Similarly, Perryman et al. (1997) quotes a proper motion of $(0.41, -8.22)$ mas/yr.

We have used the second release of the USNO CCD Astrograph Catalog (UCAC2; Zacharias et al. 2004) project to illustrate the cluster proper motion. Figure 1 displays the vector point diagrams (proper motion in right ascension versus proper motion in declination) for all stars within two degrees in radius from the cluster centre for magnitude brighter than 9.0, 10.0, and 11.0, respectively. Two clustering of stars emerge from these diagrams. Similarly, two peaks are also seen when plotting the histogram of the number of stars as a function of declination for magnitudes brighter than 10.0 mag. (Fig. 2). The first group of stars has no significant proper motion and denotes field stars whereas the second exhibits a shift in declination and corresponds to the cluster. In addition, we have included the vector point diagram for a control field (RA = 17^h08 , dec = $+9^\circ$) over a 2 degrees in radius and for UCAC2 magnitudes brighter than 9.0. The comparison of this diagram with the top left one in Fig. 1 reveals an overdensity of stars at expected proper motion for Collinder 359. The top right his-

togram in Fig. 2 shows that the number of sources at $\mu_\delta \sim -8.0$ mas/yr exceeds the number of objects with a zero proper motion, confirming hence the presence of a cluster.

2.2. The age of the cluster

Wielen (1971) derived an age of 20–50 Myr with a mean value of 30 Myr by fitting isochrones in three-colour photometry obtained from large catalogues of open clusters (Becker & Fenkart 1971). Abt & Cardona (1983) studied the distribution of Ap stars in open clusters as a function of age and put an upper limit of 30 Myr on the age of Collinder 359, assuming that 67 Oph is a member of the cluster. Both results are in agreement and consistent with the most recent estimate from Kharchenko et al. (2004; personal communication).

We have attempted to estimate the age of Collinder 359 and its associated error using its most massive members. We have followed the approach applied to α Per by Stauffer et al. (2003). By comparing the location of the star α Persei (open square in Fig. 3) in the colour-magnitude diagram ($B - V, M_V$) with theoretical solar metallicity isochrones including moderate overshoot (Girardi et al. 2000), an age of 50 Myr was inferred for α Per (dot-dashed line in Fig. 3). We should keep in mind that the lithium test applied to the α Per cluster yielded a value larger than the turn-off main-sequence method (90 Myr versus 50 Myr; Stauffer et al. 1999).

Collinder 359 is located around the B5 supergiant, 67 Oph (filled circle in Fig. 3), which is considered as a member of the cluster with a probability of 75% and over 95% by Baumgardt et al. (2000) and Kharchenko et al. (2004), respectively.

Assuming a mean apparent magnitude of $V = 3.96 \pm 0.02$ and a mean distance of 435^{+220}_{-110} pc (Perryman et al. 1997), we have derived an absolute magnitude of $M_V = -4.23^{+0.63}_{-0.89}$. The

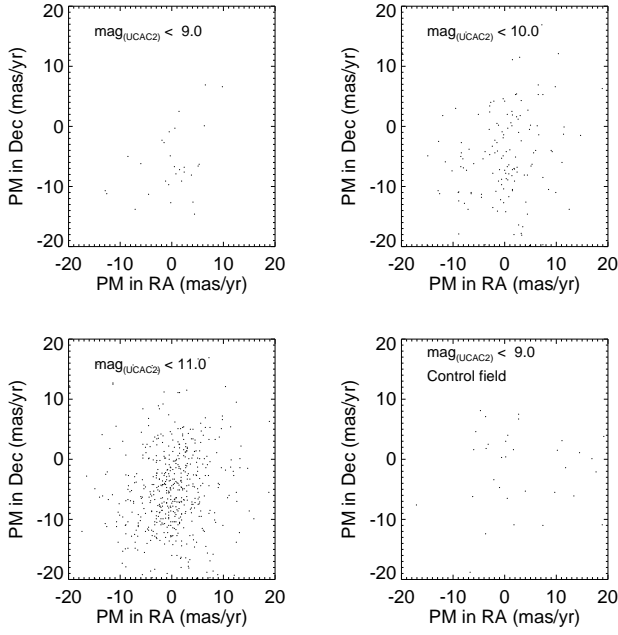


Fig. 1. Vector point diagrams for all stars within two degrees in radius from the cluster centre for magnitudes brighter than 9, 10, and 11, respectively. The bottom right displays the vector point diagram from a control field (RA = 17^h08, dec = +9°). The proper motions (accurate to 6 mas/yr) are taken from the USNO CCD Astrograph Catalog (Zacharias et al. 2004). Two clusterings are clearly separated for magnitudes brighter than 10.0. The first is located at (0,0), and the second at approximately (0.0, −8.5) mas/yr in right ascension and declination, respectively. The comparison between the cluster and controls fields at bright magnitudes depicts the presence of an overdensity of sources with a proper motion consistent with Collinder 359.

vertical line crossing the circles in Fig. 3 represents the uncertainty on the parallax estimate of 67 Oph. The best positional fit of 67 Oph in the ($B - V$, M_V) colour-magnitude diagram is obtained for an age of 60 Myr (between the dot-dashed and dotted lines in Fig. 3), with an uncertainty of 20 Myr (extent of the vertical line). Our age estimate is twice the value of 30 Myr quoted by Wielen (1971) but larger than the main-sequence turn-off age of the α Per cluster, suggesting that Collinder 359 is likely older than α Per but younger than the Pleiades. We note that more recent age determination in open clusters using the lithium test (Rebolo, Martín, & Magazzù 1992) led to older ages by a factor of ~ 1.6 than the turn-off main-sequence method (Jeffries & Naylor 2001). The age of Collinder 359 could therefore be as old as 100 Myr.

2.3. The distance of the cluster

Based on isochrone fitting of early-type stars, Collinder (1931) derived a distance ranging from 210 pc to 290 pc for Collinder

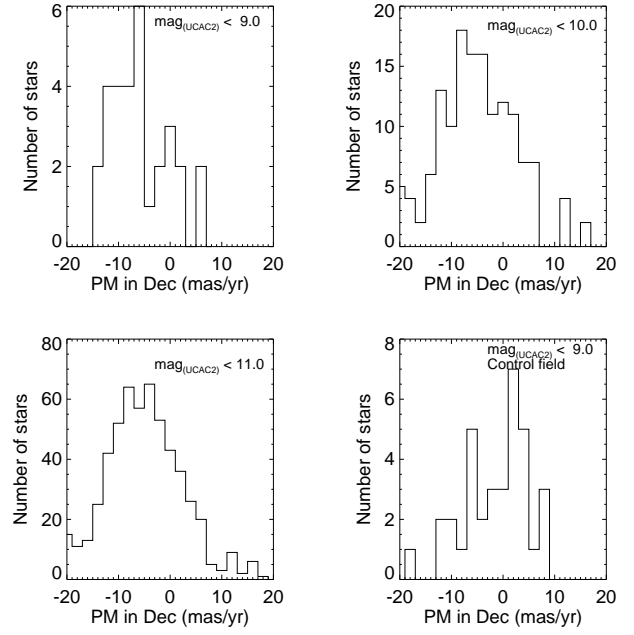


Fig. 2. Histograms of the number of sources as a function of declination for all stars located within two degrees in radius from the cluster centre for magnitudes brighter than 9, 10, and 11, respectively. We have added a vector point diagram for a control field over a 2 degree radius centred on RA = 17^h08 and dec = +9° (bottom right). The proper motions are from the UCAC catalogue (Zacharias et al. 2004) and accurate to 6 mas/yr. The presence of the cluster is inferred from the comparison of the top left and bottom right histograms. The top right histogram shows an overdensity of sources at $\mu_\delta \sim -8.0$ mas/yr.

359. Following new photometric studies by Van't-Veer (1980) and Rucinski (1980, 1987), the rejection of some objects originally proposed as cluster members yielded a revised distance of 436 pc. In the 5th Open Cluster Data Catalogue (Lyngå 1987), a distance of 200 pc was quoted based on the Bochum-Strasbourg magnetic tape catalogue of open clusters. The HIPPARCOS parallax measurement of the supergiant 67 Oph led to a distance of 435^{+220}_{-110} pc (Perryman et al. 1997). Trigonometric parallaxes of five photometric members from HIPPARCOS yielded distances between 260 and 280 pc for Collinder 359 (Loktin & Beshenov 2001). Combining the HIPPARCOS and Tycho 2 catalogues, a list of about 100 possible cluster members (open squares in Fig. 4) were extracted by Kharchenko et al. (2004, personal communication) based on their location within the cluster area and their proper motions. The position of these objects in the ($B - V$, V) colour-magnitude diagram yielded a distance of 650 pc from isochrone fitting.

To summarise, the distance of Collinder 359 is not well constrained to date. We will adopt a mean distance of 450 pc with an uncertainty of 200 pc (Table 2).

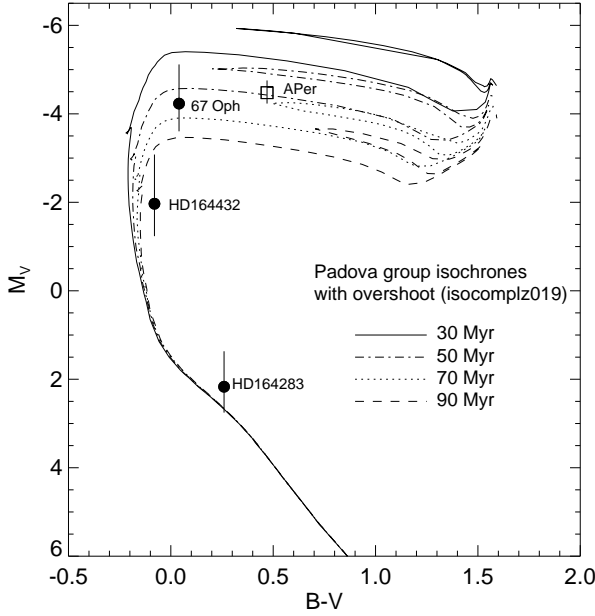


Fig. 3. $(B - V, M_V)$ colour-magnitude diagram. The position of the F5 supergiant Alpha Per (open square), the B5 supergiant 67 Oph, HD164432 (B3), and HD164283 (A0) (filled circles) are indicated. Overplotted are the solar metallicity evolutionary models with moderate overshoot from the Padova group (Girardi et al. 2000) for 30 Myr (solid line), 50 Myr (dot-dashed line), 70 Myr (dotted line), and 90 Myr (dashed line). The vertical line crossing the solid circles represent the errors on the HIPPARCOS parallax for 67 Oph (Perryman et al. 1997). The best fit is obtained for ages of 50 Myr and 60 Myr for the α Per and Collinder 359 clusters, respectively.

Table 2. Method and references for the various distance estimates for the open cluster Collinder 359. In this paper, we adopt a mean distance of 450 pc with an uncertainty of 200 pc.

Method	d (pc)	reference
Isochrone fitting	210–290	Collinder (1931)
Isochrone fitting	436	Rucinski (1987)
Isochrone fitting	200	Lyngå 1987
Parallax (HIPPARCOS)	435^{+220}_{-110}	Perryman et al. (1997)
Parallax (HIPPARCOS)	260–280	Loktin & Beshenov (2001)
Isochrone + proper motion	650	Kharchenko et al. 2004

3. The CFHT Key Programme

We have carried out a CFHT Key Programme (30 nights over 2 years) centred on wide-field optical imaging in a variety of environments to examine the sensitivity of the low-mass stellar and substellar IMF to time and environment. This work was conducted within the framework of the European Research Training Network “The Formation and Evolution of Young Stellar Clusters”. Other goals were to address the most pressing issues concerning low-mass stars and BDs, including their formation, their distribution, and their evolution with time.

The survey was conducted with a large-CCD mosaic camera (CFH12K) in the I and z filters down to detection and completeness limits of $I = 24.0$ and 22.0 mag, respectively, covering a total of 80 square degrees in star-forming regions, open clusters, and in the Hyades.

The CFH12K is a CCD mosaic camera dedicated to high-resolution wide-field imaging. The camera comprises 12 chips of 4128×2080 pixels with a pixel scale of 0.206 arcsec, yielding a field-of-view of 42×28 arcmin. Hence, no problem of undersampling was foreseen even during excellent conditions on Mauna Kea, which was the case for our observations. The cosmetics of the CFH12K mosaic was excellent with a total of 200 bad columns, most of them were concentrated on CCD05. The CCD06, CCD08, CCD09, CCD10, and CCD11 are entirely free of bad columns.

We have chosen to carry out the wide-field optical observations in the I and z filters mainly to optimise the search for low-mass stars and BDs in young clusters. This choice was also motivated by the results of a 6.4 square degree imaging survey of the Pleiades with the CFH12K in the I - and z -bands (Moraux et al. 2003) conducted with the same telescope/instrument configuration. Numerous brown dwarf candidates in the Pleiades were discovered down to $30 M_{\text{Jup}}$. The derived mass function was in agreement by that determined by Bouvier et al. (1998). Moreover, the empirical knowledge of the mass function was extended far into the substellar regime.

4. The wide-field optical survey in Collinder 359

4.1. Observations and data reduction

Five CFH12K frames were obtained on 18 and 20 June 2002 in Collinder 359 in the I and z filters, covering a total area of 1.6 square degrees in the cluster (Table 3). Figure 4 displays the location of the five CFH12K pointings within the cluster area and Table 3 gives the journal of the observations. Thirteen possible members as listed by Collinder (1931) (filled circles in Fig. 4) are also overplotted. The CFH12K frames were chosen to avoid bright cluster members. These frames are located about half a degree away from the cluster centre and have a small overlap with the possible members extracted by Kharchenko et al. (2004; personal communication).

Table 3. Coordinates (J2000) of the five CFH12K fields-of-view ($42 \text{ arcmin} \times 28 \text{ arcmin}$) along with the journal of observations obtained in the pre-main-sequence open cluster Collinder 359. The times of observations are given in UT and correspond to the beginning of the short exposures in the I -band.

Field	R.A.	Dec	Obs. Date	Time of obs.
A	18 01 06.6	+02 07 26	2002–06–18	08h19m15s
B	18 02 36.9	+03 37 52	2002–06–18	09h07m43s
C	17 57 36.9	+03 37 56	2002–06–18	09h56m07s
D	17 56 16.4	+02 29 46	2002–06–18	11h52m24s
E	18 05 55.7	+03 28 58	2002–06–20	12h29m20s

Fields A, B, C, and D were obtained on 18 June 2002 under photometric conditions with seeing ~ 0.8 arcsec. The remaining field, field E, was observed on 20 June 2002 under non-photometric conditions (extinction less than 0.05 mag at the time of the observations; see atmospheric attenuation on the Elixir webpage²). Three sets of exposures were taken for each field-of-view: short, medium, and long exposures with integration times of 2, 30, and about 900 seconds, respectively. The long exposures consisted of three times 300 and 360 seconds in the *I* and *z* filter, respectively, yielding detection limits of 24.0 mag in both passbands. Only one image was taken for the short and medium exposures, whereas three dithered positions were obtained for the long exposures, allowing rejection of bad pixels and removal of bad columns. The observations were scheduled in a queue mode so that the short, medium, and long exposures in the *I*-band were taken immediately prior to the short, medium, and long exposures in the *z*-band.

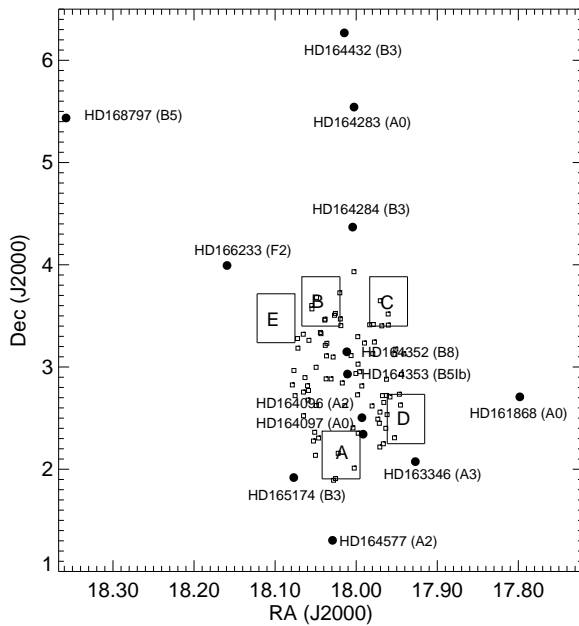


Fig. 4. Location of the five CFH12K fields-of-view (A, B, C, D, and E) shown as boxes within the cluster area defined by the WEBDA Database. The 13 possible cluster members listed by Collinder (1931) and given in Table 1 are displayed as filled circles. Their names and spectral types are provided as well. The open squares are possible members used for isochrone fitting by Kharchenko et al. (2004; personal communication) to derive a distance of 650 pc and an age of 30 Myr.

The initial data reduction was provided by the Elixir pipeline (Magnier & Cuillandre 2004) and includes bias subtraction, flat-fielding, correction for scattered light in the *I* and *z* bands, combining the dithered frames in case of long exposures, and astrometric solution provided in the header of the fits files. Standard stars were observed throughout the nights

and were monitored constantly by the Elixir/Skyprobe tool to provide accurate zero-points.

4.2. Optical photometry

We have used the SExtractor software³ (Bertin & Arnouts 1996) to extract the photometry from the optical images. We have favoured the point-spread function (PSF) fitting to aperture photometry because it provides more precise photometric measurements for faint sources, which are, in our case, the cluster brown dwarf candidates. We have been kindly provided the PSFex package by E. Bertin (personal communication) to carry out PSF fitting.

The data reduction procedure to extract a catalogue of all objects from the reduced and stacked images processed by the pipeline was identical for each CFH12K field-of-view. First, we have combined the *I* and *z* images to increase the signal-to-noise ratio and permit a better astrometry of faint sources close to the detection limit. Therefore, the detection of sources was run on the combined image whereas the photometry was applied to the *I*- and *z*-band images. We have run SExtractor and PSFex to extract coordinates and magnitudes for all detected sources by using a model PSF for each chip and each field. Afterwards, we have applied the zero points listed on the Elixir webpage⁴ to calibrate our photometric measurements. The nominal CFH12K zero points for the *I*- and *z*-bands were $ZP(I) = 26.184 \pm 0.023$ and $ZP(z) = 25.329 \pm 0.031$, respectively. Small corrections were applied for the nights of 18 and 20 June 2002 to take into account the weather conditions on those specific nights. Finally, the *I* and *z* catalogues were cross-correlated by matching pixel coordinates.

One catalogue was generated for each CCD chip of each CFH12K field-of-view for all three exposures (short, medium, and long). The catalogues contain the pixel and celestial coordinates, magnitudes, as well as other parameters, including the full-width-half-maximum and the ellipticity of the source. The final magnitudes (see electronic table) have rms errors on the *I*-band magnitudes smaller than 0.1 mag.

4.3. Calibration of the photometry

We have conducted a number of “checks” to verify the validity of the photometry. We have ensured that colour-magnitude diagrams of all chips in one CFH12K field-of-view align properly (see de Wit et al. 2005). To calibrate internally our photometry, we have cross-correlated the short and medium and the medium and long exposures for each individual field-of-view. We were unable to calibrate the magnitudes between fields because no overlapping area between the CFH12K pointings was available.

We have also attempted to calibrate our photometry externally. However, on the one hand, the CFH12K fields-of-view were chosen to avoid bright cluster members (Fig. 4) and, on the other hand, no previous study was conducted in those areas. Nevertheless, we have cross-correlated our final source

³ <http://astroa.physics.metu.edu.tr/MANUALS/sextractor/>

⁴ <http://www.cfht.hawaii.edu/Instruments/Elixir/stds.2003.06.html>

² <http://www.cfht.hawaii.edu/Instruments/Elixir/stds.2003.06.html>

Table 4. Catalogue of cluster member candidates in Collinder 359, assuming a distance of 450 pc and an age of 60 Myr for the cluster. The total number of sources is 506. The name of each individual target is given in the first column according to the IAU nomenclature. The CFH12K field-of-view and the identification number of each source is provided in Cols. 2 and 3. Right ascension and declination (in J2000) are listed in Cols. 4 and 5. Optical (I and z) and 2MASS near-infrared magnitudes are provided in Cols. 6–10. Finally, the membership of each target is given in the last column. Y stands for possible member whereas NM depicts a non-member of the cluster.

IAU Name	FOV	ID	R.A.	Dec	I	z	J	H	K_s	Mem?
Cr359 J175453+023353	D00	1469	17 54 53.20	02 33 53.6	11.537	11.326	10.197	9.457	9.236	Y
...
Cr359 J175507+022403	D06	5613	17 55 07.79	02 24 03.2	22.480	21.320	—	—	—	Y

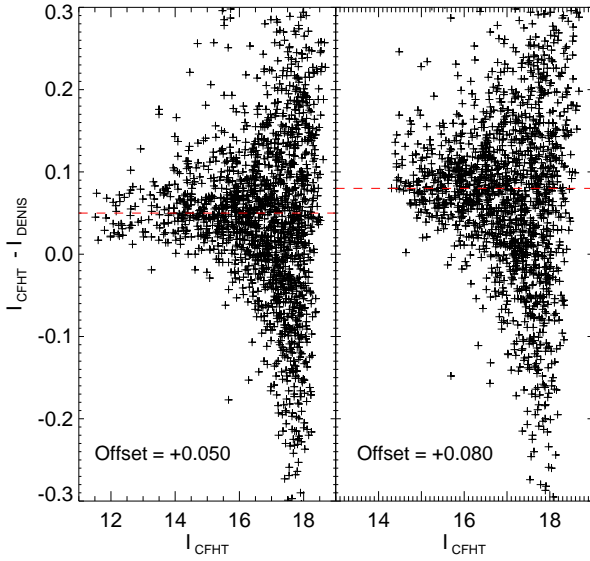


Fig. 5. Offsets in I magnitudes between the CFHT and DENIS measurements for a 15×6 arcmin overlapping area located in field A. Photometric shifts of +0.050 and +0.080 mag are found for the short (left panel) and medium (right panel) exposures, respectively. The same procedure was not possible with the deep exposures since the detection of DENIS corresponds to the saturation limit of the CFH12K long exposures.

catalogue with the recent release of the DEep Near-Infrared Survey (Epchtein et al. 1997). We could extract a small overlapping region (15×6 arcmin) between the DENIS survey and the area covered by Field A ($17^{\text{h}}59^{\text{m}}30^{\text{s}} \leq \text{RA} \leq 18^{\text{h}}02^{\text{m}}30^{\text{s}}$ and $+01^{\circ}54' \leq \text{Dec} \leq +02^{\circ}00'$). The mean photometric offsets in the I magnitudes between the CFHT and DENIS measurements are $+0.05 \pm 0.09$ and $+0.08 \pm 0.12$ mag for short and medium exposures, respectively, as shown in Fig. 5. A similar procedure could not be applied to the long exposures because the DENIS detection limit corresponds to the saturation of the CFH12K long exposures ($I = 18.0$ – 18.5 mag). The agreement between the DENIS and CFH12K magnitudes is on the order of the dispersion observed in our photometry and does not affect the subsequent candidate selection in Collinder 359. Note that the er-

rors on the DENIS magnitudes are up to 0.13, 0.18, and 0.22 mag at $I = 16, 17$, and 18 , respectively.

5. New cluster member candidates in Collinder 359

5.1. Optical colour-magnitude diagram

The final $(I - z, I)$ colour-magnitude diagram for all detections in the 1.6 square degree area surveyed in Collinder 359 is presented in Fig. 6. The detection and completeness limits of the survey are estimated to $I \sim z \sim 24.0$ and 22.0 mag, respectively. To create the final colour-magnitude diagram, we have cross-correlated the short with medium and medium with long exposures to remove common detections and keep the best photometry. Hence, the photometry of the objects with $I \leq 15.0$ mag, $15.0 \leq I \leq 19.0$ mag, and $I \geq 19.0$ mag is extracted from the short, medium, and long exposures, respectively.

Overplotted on the colour-magnitude diagram are the 60 Myr NextGen (solid line; Baraffe et al. 1998) and the DUSTY (dashed line; Chabrier et al. 2000b) isochrones, assuming a distance of 450 pc for the cluster. The horizontal dashed line at $I \sim 19.75$ mag corresponds to the hydrogen-burning limit (HBL) at $0.072 M_{\odot}$. The mass scale indicated on the right-hand side of the plot in solar masses spans $1.3 M_{\odot}$ to $0.030 M_{\odot}$. A reddening vector with $A_V = 1$ mag is indicated by an arrow for comparison purposes. We have considered an interstellar absorption law with $A_I = 0.482$ mag for the I -band (Rieke & Lebofsky 1985). As no estimate is available in the z band, we have assumed a linear fit between the interstellar absorption in the I and J bands ($A_J = 0.282$ mag), yielding $A_z = 0.382$ mag.

5.2. Selection of cluster member candidates

The extraction of member candidates in open clusters generally consists in selecting objects located to the right of the ZAMS (Leggett 1992) shifted to the distance of the cluster. We have chosen the evolutionary models from the Lyon group to select candidates in Collinder 359. We have employed the NextGen isochrones (solid line in Fig. 6; Baraffe et al. 1998) for effective temperatures higher than 2500 K (corresponding to $0.050 M_{\odot}$ at the age and distance of the cluster) and the DUSTY (dashed line in Fig. 6; Chabrier et al. 2000b) isochrones for lower temperatures (and masses). We did not consider the Cond models since the isochrone lie to the right of the DUSTY

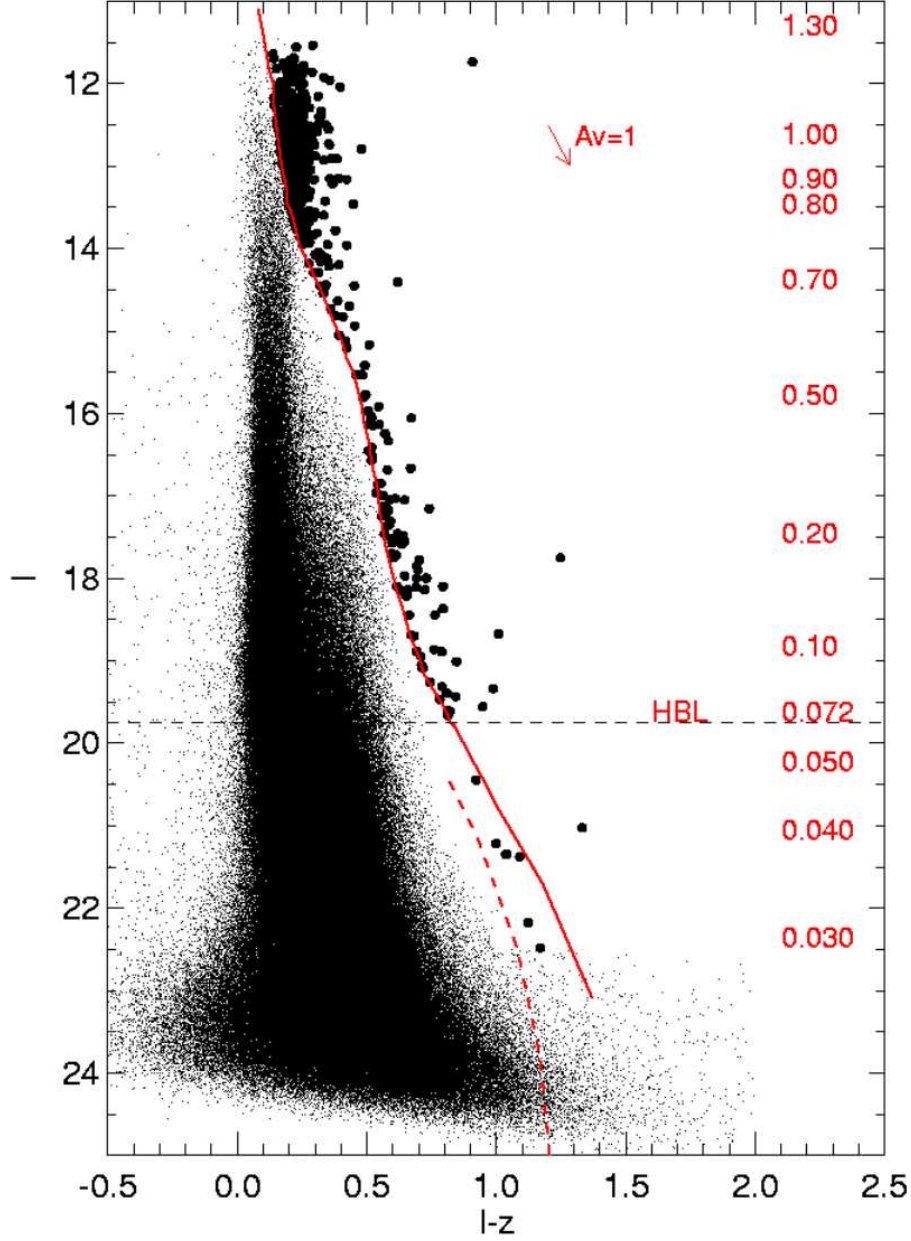


Fig. 6. Colour-magnitude diagram ($I - z, I$) for the intermediate-age open cluster Collinder 359 over the full 1.6 square degree area surveyed by the CFH12K camera. The large filled dots are all optically-selected cluster member candidates spanning $1.3\text{--}0.03\text{ M}_{\odot}$, assuming an age of 60 Myr and a distance of 450 pc. Overplotted are the NextGen (solid line; Baraffe et al. 1998) and the DUSTY (dashed line; Chabrier et al. 2000b) isochrones for 60 Myr, assuming a distance of 450 pc for the cluster. The dashed line at $I \sim 19.75$ mag indicates the hydrogen-burning limit (HBL) at 0.072 M_{\odot} . The mass scale (in M_{\odot}) is given on the right side of the graph for the assumed age and distance for the cluster. A reddening vector of $A_V = 1$ mag is indicated for comparison purposes.

isochrone. Consequently, objects located to the right of the Cond isochrones are to the right of the DUSTY isochrones as well and, hence, remain bona-fide cluster member candidates. We have selected *all* objects located to the right of the combined NextGen+DUSTY isochrones, assuming a distance of 450 pc and an age of 60 Myr for Collinder 359.

We have examined each cluster candidate by eye both in the I and z images to reject extended objects, blended sources, and detections affected by bad pixels or bad columns. Indeed, more than two-thirds of the objects located to the right of the evolutionary models were affected by bad pixels in one filter at

least, or located on a bad column despite the good cosmetics of the CFH12K camera.

After removal of all spurious detections, the final list of cluster members contains a total of 506 candidates ranging from $I = 11.3$ to $I = 22.5$ mag over 1.6 square degree area surveyed in Collinder 359 (Table 4). Column 1 gives the name of the target according to the IAU convention. We used the name Coll359J to refer to Collinder 359 followed by the coordinate in J2000. Columns 2 and 3 provide the field-of-view where the candidate is located and the identification number assigned during the extraction of the photometry. Cols. 4 and 5 list the right ascension (in hours) and declination (in degrees) of the objects extracted from the CFH12K images (in J2000). Cols. 6–11 give the optical (I and z) and the near-infrared (J , H , and K_s) magnitudes. Column 12 provides an update of the membership status of the candidate after considering the near-infrared follow-up, where Y stands for possible members and NM for non-members.

The range of ellipticities and full-width-half-maxima for all candidates are 0.001–0.265 and 1.6–3.2, respectively. Only one object has an ellipticity of 0.602 and a FWHM of 2.8, casting doubt about its membership. The distribution of ellipticities shows that 95 % of the objects have an ellipticity smaller than 0.15. The majority of objects have FWHM between 1.8 and 3.0, corresponding to a seeing of ~ 0.4 – 0.6 arcsec.

It is possible that we have missed some bona-fide cluster members for various reasons. Our detection rate was not 100 % nor was our completeness limit sufficiently deep to have detected all members. Additionally, we did not detect the bright cluster members due to our saturation limit at about $I = 12$ mag. Second, 200 bad columns affect the CFH12K field-of-view and most especially the CCD05 where the largest incompleteness is expected. Similarly, objects affected by bad pixels might actually be genuine cluster candidates but were rejected from the final list because of their dubious photometry. Source blending represents another effect which prevents us from detecting all members. Last but not least, we did not cover the whole cluster, implying that there are other, potentially large numbers of members yet to be discovered.

From the colour-magnitude diagram ($I - z, I$), the large field contamination at magnitudes brighter than $I \sim 14$ mag is clearly visible. Out of the 506 candidates, 70 % of them lie in the range $I = 12$ – 14 mag. The large number of candidates at brighter magnitudes (and thus at high masses) originates from the merging between the cluster sequence and the sequence of field stars. There is likely to be considerable field star contamination in this mass range for the cluster as seen in the colour-magnitude diagram.

If we consider an age of 100 Myr as suggested by recent age determination in open clusters using the lithium test (Stauffer et al. 1999), the number of candidates increases to 628 in the same magnitude range. According to evolutionary isochrones (Baraffe et al. 1998), the stellar/substellar boundary would then be at $I = 20.2$ mag, half a magnitude fainter than at 60 Myr.

6. Near-infrared photometry follow-up of optically-selected candidates

Collinder 359 is at a Galactic latitude of $|b| = 12.5^\circ$, intermediate between α Per ($|b| = 7^\circ$) and the Pleiades ($|b| = 24^\circ$). Therefore, the sample of optically-selected cluster member candidates in Collinder 359 is inevitably contaminated by foreground and background objects, including galaxies, reddened background giants, and field dwarfs.

We took special care in the removal of extended objects from the cluster candidate list so that we expect a small contamination by background galaxies. Field dwarfs also represent another source of contamination as they have similar optical colours as young cluster members. However, optical-to-infrared colour-magnitude diagrams such as ($I - J, I$) or ($I - K_s, I$) have proven their efficiency in weeding out field dwarfs in σ Orionis (Zapatero Osorio et al. 2000), in the Pleiades (Zapatero Osorio et al. 1997; Pinfield et al. 2000) in α Per (Barrado y Navascués et al. 2002), and in IC 2391 (Barrado y Navascués et al. 2001b). Furthermore, the latest theoretical DUSTY isochrones (Chabrier et al. 2000a) predict bluer $I - K$ colours for field dwarfs than young low-mass cluster members by 1.0 to 1.5 mag depending on the mass.

6.1. Cross-correlation with the 2MASS database

To estimate the contamination towards bright member candidates in Collinder 359, we have cross-correlated the sample of optically-selected cluster member candidate with the 2MASS All-Sky release catalogue of point-sources (Cutri et al. 2003)⁵. Due to its completeness limit of $K_s = 14.3$ mag, the 2MASS database provides infrared counterparts in J , H , and K_s for most of the optically-selected cluster candidates brighter than $I = 17.0$ mag. For objects fainter than $K_s = 14.3$ mag, the uncertainty on the magnitude become larger than 0.1 mag and additional near-infrared observations are required to establish membership.

Among 433 cluster member candidates brighter than 17.0 mag in the I -band, 426 of them have a 2MASS counterpart within a radius of 2 arcsec, with $K_s < 14.3$, and errors on the J , H , and K_s magnitudes smaller than 0.1 mag. Robust near-infrared photometry is available for 97 % of our sample to $I = 17$ mag. The remaining objects have a 2MASS counterpart but either at larger radii (2 to 3 arcsec) or K_s magnitudes fainter than 14.3 or uncertainties larger than 0.1 mag. We have therefore not considered their 2MASS magnitudes but obtained additional photometry for half of them.

6.2. Additional near-infrared photometry

We have carried out near-infrared photometry for fainter objects to probe the contamination at lower masses and across the stellar/substellar boundary.

Near-infrared (K' -band) photometry was obtained for 29 optically-selected candidates on 10–12 July 2003 with the CFHTIR infrared camera. This camera has a 1024×1024 pixel

⁵ <http://www.ipac.caltech.edu/2mass/releases/second/doc/>

HAWAII detector with a spatial scale of $0.204''/\text{pixel}$ yielding a 3.5×3.5 arcmin field-of-view. The total exposure time was on the order of 5 minutes per object and the photometric errors better than 0.1 mag.

Additional infrared photometry (K_s -band) was obtained for 36 candidates on 10–13 June 2004 with MAGIC on the Calar Alto 2.2-m telescope. The MAGIC camera has a Rockwell 256×256 pixel NICMOS3 array with a spatial scale of $0.64''/\text{pixel}$ yielding a $164''$ field-of-view in the high-resolution mode when mounted on the 2.2-m. Five dithered frames offset by about 25 pixels were taken for each target, yielding exposure times between 20 and 120 seconds depending on the brightness of the target.

The infrared data was reduced following standard procedures. First, a sky image was created using a median of the dithered frames. Then, each science frame was sky-subtracted and flat-fielded. The flat-field is the difference between averaged dome flat fields observed lamp on and lamp off. The measured magnitudes were corrected for extinction and exposure time. The airmass correction was assumed to be 0.07 and 0.088 mag/airmass for Mauna Kea and Calar Alto, respectively. Zero-points from the various standards observed throughout the nights were applied to the instrumental magnitudes and cross-checked with 2MASS to derive the final magnitudes.

7. Contamination of the optical sample

7.1. Near-infrared photometry

Figure 7 shows the location of the optically-selected candidates in Collinder 359 in an optical-to-infrared colour-magnitude diagram ($I-K, I$). Objects with 2MASS magnitudes are displayed with a plus sign while targets from our own near-infrared follow-up observations are shown as filled circles. The solid and dashed lines represent the 60 Myr NextGen and DUSTY isochrones, respectively, at a distance of 450 pc. The isochrones are drawn using the I filter from the CFH12K camera and the K_s filter from 2MASS (I. Baraffe, personal communication). Note that the K' and K_s magnitudes are very similar and do not affect the results concerning the membership of the candidates.

According to their location in the ($I-K, I$) diagram, cluster candidates are divided into two subsamples as follows:

1. Probable members (Y+): these objects lie to the right of the NextGen+DUSTY isochrones, shifted at a distance of 450 pc. Their colours are consistent with cluster membership.
2. Non-members (NM): objects with colours bluer than those predicted by the isochrones shifted at a distance of 450 pc.

Combining the optical and optical-to-infrared colour-magnitude diagrams, most of the candidates brighter than $I = 17.0$ mag remain possible candidates. Indeed, only 9 out of 433 are rejected as cluster members, yielding a contamination on the order of few percent. This simple analysis is however inadequate. Both colour-magnitude diagrams show a wide cluster sequence at $I \leq 14$ mag, suggesting a large contamination by red field stars. Using our current data we are unable to estimate the contamination properly in this magnitude range. Ultimately, low-resolution optical spectroscopy will provide

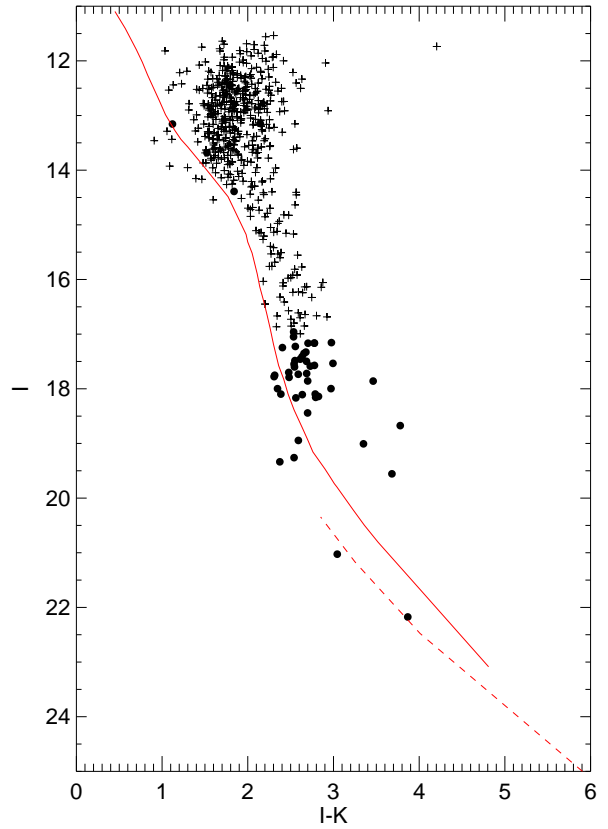


Fig. 7. Colour-magnitude diagram ($I-K, I$) for the optically-selected candidates in Collinder 359. The plus symbols denotes candidates with 2MASS photometry whereas the filled circles have been observed with the CFHTIR and MAGIC cameras. Overplotted are NextGen (solid line; Baraffe et al. 1998), and the DUSTY (dashed line; Chabrier et al. 2000b), assuming an age of 60 Myr and a distance of 450 pc for Collinder 359.

additional constraints, including lithium, radial velocities, and spectral types, to distinguish field stars from cluster members.

At fainter magnitudes, the cluster sequence becomes clearer and extends down to $I = 22$ mag in the optical colour-magnitude diagram. From the optical-to-infrared colour-magnitude diagram, we rejected 6 optically-selected cluster candidates out of 42 in the magnitude range $I = 17-22$ mag, yielding a contamination of $\sim 14\%$ across the stellar/substellar boundary. It is hard to set limits on the contamination at present due to the small number statistics across the stellar/substellar boundary. We are still lacking photometry for cluster candidates fainter than $I = 17$ mag.

7.2. Statistical contamination from a control field

We now estimate the statistical contamination from a control field observed within the framework of the CFH12K optical survey conducted in IC 4665 (de Wit et al. 2005). The control field coordinates are R.A. = $17^{\text{h}}40^{\text{m}}53^{\text{s}}$ and dec = $+02^{\circ}50'14''$ corresponding to a Galactic latitude of $b = +17^{\circ}$ similar to

IC 4665 but higher than Collinder 359 ($b = +12.5^\circ$). The study of IC 4665 reveals a contamination of 85 % and 70 % in the low-mass and brown dwarf regimes, respectively (see de Wit et al. 2005, for more details). Those figures are likely lower limits for Collinder 359 due to its lower Galactic latitude and larger distance compared to IC 4665 (450 pc vs. 350 pc).

8. IC 4665 & Collinder 359: a larger picture

The open clusters Collinder 359 and IC 4665 are very close on the sky, their centres being about 5 degrees apart (Fig. 8). Additionally, they share the same proper motion ($0.0, -9.0$ mas/yr; Perryman et al. 1997), have similar ages (50–100 Myr) and comparable distance estimates within the uncertainty errors (450 vs. 350 pc).

We have selected all sources brighter than $V = 10.5$ mag in a 10×10 degrees area encompassing Collinder 359 and IC 4665 using archival data from the ASCC2.5 catalogue (Kharchenko 2001). This catalogue is a compilation of high-precision catalogues from space missions, including HIPPARCOS and Tycho-2, and ground-based proper motions surveys providing coordinates, accurate proper motions, and photometry. Sources located with a 2.5 mas/yr radius and centred on $(0.0, -9.0)$ mas/yr in right ascension and declination, respectively, define two clusterings (filled circles in Fig. 8) at the nominal cluster centres. In comparison, objects with proper motion of -3.0 and 0.0 mas/yr in right ascension and declination, respectively, are randomly distributed over the same area (squares in Fig. 8), implying that we have indeed two clusters.

We have examined the number of objects located within a 2 degree box around each cluster. We have found 15 and 19 sources (filled circles in Fig. 8) in IC 4665 and Collinder 359, respectively, and a total of 2 and 7 field dwarfs (open squares in Fig. 8) in the same area around each cluster. From the photometry point of view, 15 and 16 sources have $B - V < 1.0$ in IC 4665 and Collinder 359, respectively. The number of field dwarfs with $B - V < 1.0$ falls down to 1 and 4, respectively. Moreover, the objects in Collinder 359 do not defined a sequence in the $(B - V, V)$ colour-magnitude diagram as clear as the members of IC 4665 do (Fig. 9). The lack of clear sequence in the colour-magnitude diagram and the larger number of contaminants towards the line of sight of Collinder 359 tend to suggest that this cluster is much less massive than IC 4665. Nevertheless, the shift present between both sequences could well be assigned to an extinction of ~ 0.1 mag as the region exhibit signs of variable extinction. Moreover, Collinder 359 might not be a real cluster but either linked to IC 4665 or a moving group associated to the Ophiuchus cloud (Röser & Bastian 1994). A survey of the inner region of the cluster i.e. within 1 degree radius of the cluster centre is required to answer those issues and determine the characteristics of Collinder 359.

9. Summary

We have presented the first deep optical wide-field imaging survey complemented with near-infrared photometric observations of the young open cluster Collinder 359. We have surveyed a 1.6 square degree area in the cluster in the I and z

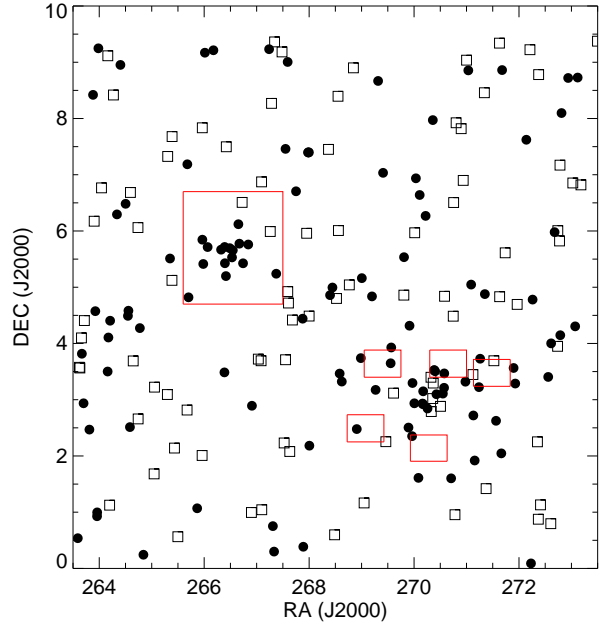


Fig. 8. Sources brighter than $V = 10.5$ mag with proper motion from the ASCC2.5 (Kharchenko 2001) over a 100 square degree area encompassing IC 4665 and Collinder 359. Filled circles correspond to sources with a proper motion consistent with the cluster motions $(0.0, -9.0)$ mas/yr. Open squares are sources with a random motion. The filled circles are grouped into two clusterings whereas open squares are randomly distributed over the 10 by 10 degree area. The black boxes correspond to our CFH12K coverage of the open clusters Collinder 359 and IC 4665.

filters down to detection and completeness limits of 22.0 and 24.0 mag with the CFH12K wide-field camera on the Canada-France-Hawaii 3.6-m telescope. Based on their location in the optical $(I - z, I)$ colour-magnitude diagram, we have extracted a total of 506 cluster member candidates in Collinder 359 spanning $1.3\text{--}0.030 M_\odot$, assuming a distance of 450 pc and an age of 60 Myr. The uncertainties on the distance and age are 200 pc and 20 Myr, respectively. We have cross-correlated the optically-selected candidates with the 2MASS database for objects brighter than $I = 17.0$ mag to weed out a proportion of contaminating field stars. Further K' -band photometry has been obtained for a subsample of 49 faint cluster candidates to probe the contamination at and below the stellar/substellar boundary.

By comparing the location of the brightest cluster member 67 Oph, with solar metallicity isochrones including moderate overshoot, we have derived an age of 60 ± 20 Myr for Collinder 359. Taking into account the observed differences in ages of open clusters between the turn-off main-sequence method and the lithium test, Collinder 359 is likely older than α Per but younger than the Pleiades. Thus, the expected age of the cluster is at least twice larger than previously thought. Finally, the comparison of the number of sources in a control field with the number of selected cluster candidates indicates that the surveyed fields do not contribute significantly to the cluster pop-

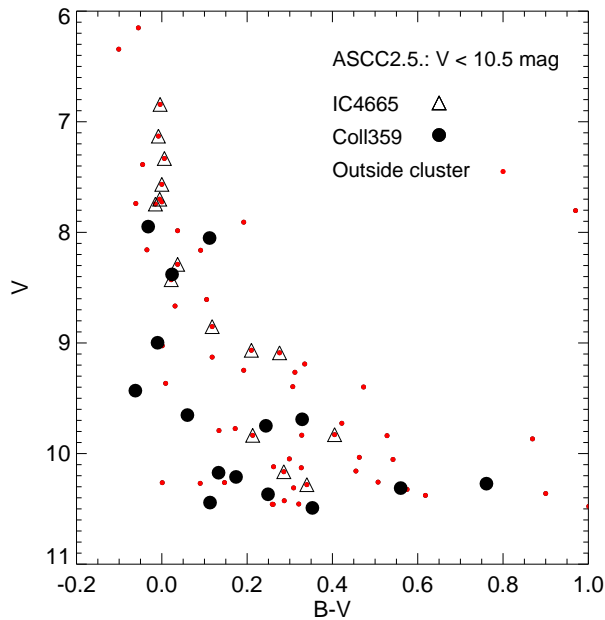


Fig. 9. Colour-magnitude diagram ($B - V, V$) for sources located within a two degrees box around the cluster centres and with a proper motion consistent with IC 4665 (open triangles) and Collinder 359 (filled circles). The small circles represent the objects with proper motion similar to the two open clusters but outside the two degree boxes around each cluster centre.

ulation. A new optical survey closer to the cluster centre but avoiding bright stars is needed to assess its extent and properties.

Acknowledgements. This CFHT Key Programme (Bouvier, PI) was conducted within the framework of the European Research Training Network (McCaughrean, coordinator) entitled “The Formation and Evolution of Young Stellar Clusters” (HPRN-CT-2000-00155) which we acknowledge for support. NL acknowledge funding from PPARC UK in the form of a research associate postdoctoral position. NL thank Nina Kharchenko and Anatoly Piskunov for useful discussion on Collinder 359 during their stay at the AIP in Potsdam in spring 2004. We are grateful to Isabelle Baraffe for providing us with the NextGen and DUSTY models for the CFHT filters and Emmanuel Bertin for supplying the PSFex package. The authors wish to extend special thanks to those of Hawaiian ancestry on whose sacred mountain we are privileged to be guests. This research has made use of the Simbad database, operated at the Centre de Données Astronomiques de Strasbourg (CDS), and of NASA’s Astrophysics Data System Bibliographic Services (ADS). This research has also made use of data products from the Two Micron All Sky Survey, which is a joint project of the University of Massachusetts and the Infrared Processing and Analysis Center, funded by the National Aeronautics and Space Administration and the National Science Foundation.

References

Abt, H. A. & Cardona, O. 1983, *ApJ*, 272, 182
 Apai, D., Pascucci, I., Henning, T., et al. 2002, *ApJL*, 573, L115

Armitage, P. J. & Bonnell, I. A. 2002, *MNRAS*, 330, L11
 Baraffe, I., Chabrier, G., Allard, F., & Hauschildt, P. H. 1998, *A&A*, 337, 403
 Baraffe, I., Chabrier, G., Barman, T. S., Allard, F., & Hauschildt, P. H. 2003, 402, 701
 Barrado y Navascués, D., Bouvier, J., Stauffer, J. R., Lodieu, N., & McCaughrean, M. J. 2002, *A&A*, 395, 813
 Barrado y Navascués, D., Stauffer, J. R., Bouvier, J., & Martín, E. L. 2001a, *ApJ*, 546, 1006
 Barrado y Navascués, D., Stauffer, J. R., Briceño, C., et al. 2001b, *ApJS*, 134, 103
 Bate, M. R., Bonnell, I. A., & Bromm, V. 2002, *MNRAS*, 332, L65
 Baumgardt, H., Dettbarn, C., & Wielen, R. 2000, *A&AS*, 146, 251
 Becker, W. & Fenkart, R. 1971, *A&AS*, 4, 241
 Beichman, C. A., Chester, T. J., Skrutskie, M., Low, F. J., & Gillett, F. 1998, *PASP*, 110, 480
 Bertin, E. & Arnouts, S. 1996, *A&AS*, 117, 393
 Blanco, V. M., Demers, S., Douglass, G. G., & Fitzgerald, M. P. 1968, *Publications of the U.S. Naval Observatory Second Series*, 21
 Boss, A. P. 2000, *ApJL*, 536, L101
 Bouvier, J., Stauffer, J. R., Martín, E. L., et al. 1998, *A&A*, 336, 490
 Bouy, H., Brandner, W., Martín, E. L., et al. 2003, *AJ*, 126, 1526
 Briceño, C., Luhman, K. L., Hartmann, L., Stauffer, J. R., & Kirkpatrick, J. D. 2002, *ApJ*, 580, 317
 Burgasser, A. J., Kirkpatrick, J. D., Brown, M. E., et al. 2002, *ApJ*, 564, 421
 Burgasser, A. J., Kirkpatrick, J. D., Reid, I. N., et al. 2003, *ApJ*, 586, 512
 Chabrier, G., Baraffe, I., Allard, F., & Hauschildt, P. 2000a, *ApJL*, 542, L119
 —. 2000b, *ApJ*, 542, 464
 Close, L. M., Siegler, N., Freed, M., & Biller, B. 2003, *ApJ*, 587, 407
 Collinder, P. 1931, *Annals of the Observatory of Lund*, 2, 1
 Cruz, K. L., Reid, I. N., Liebert, J., Kirkpatrick, J. D., & Lowrance, P. J. 2003, *AJ*, 126, 2421
 Cutri, R. M., Skrutskie, M. F., van Dyk, S., et al. 2003, *2MASS All Sky Catalog of point sources*, 2246
 de Wit, W. J., Bouvier, J., Palla, F., et al. 2005, *A&A*, accepted (astroph.11175)
 Delgado-Donate, E. J., Clarke, C. J., & Bate, M. R. 2003, *MNRAS*, 342, 926
 Dobbie, P. D., Kenyon, F., Jameson, R. F., Hodgkin, S. T., Pinfield, D. J., & Osborne, S. L. 2002a, *MNRAS*, 335, 687
 Epchtein, N., de Batz, B., & Capovani, L. e. 1997, *The Messenger*, 87, 27
 Girardi, L., Bressan, A., Bertelli, G., & Chiosi, C. 2000, *A&AS*, 141, 371
 Gizis, J. E., Reid, I. N., Knapp, G. R., et al. 2003, *AJ*, 125, 3302
 Jayawardhana, R., Ardila, D. R., Stelzer, B., & Haisch, K. E. 2003, *AJ*, 126, 1515
 Jeffries, R. D. & Naylor, T. 2001, in *ASP Conf. Ser. 243: From Darkness to Light: Origin and Evolution of Young Stellar*

- Clusters, eds. T. Montmerle & P. André (San Francisco), p 633
- Jeffries, R. D., Thurston, M. R., & Hambly, N. C. 2001, *A&A*, 375, 863
- Kharchenko, N. V. 2001, *Kinematika i Fizika Nebesnykh Tel*, 17, 409
- Kirkpatrick, J. D., Reid, I. N., Liebert, J., et al. 1999, *ApJ*, 519, 802
- Kirkpatrick, J. D., Reid, I. N., Liebert, J., et al. 2000, *AJ*, 120, 447
- Klein, R., Apai, D., Pascucci, I., Henning, T., & Waters, L. B. F. M. 2003, *ApJL*, 593, L57
- Klessen, R. S. 2001, *ApJ*, 556, 837
- Kroupa, P. 2002, *Science*, 295, 82
- Kroupa, P., Bouvier, J., Duchêne, G., & Moraux, E. 2003, *MNRAS*, 346, 354
- Kroupa, P., Tout, C. A., & Gilmore, G. 1993, *MNRAS*, 262, 545
- Leggett, S. K. 1992, *ApJS*, 82, 351
- Lin, D. N. C., Laughlin, G., Bodenheimer, P., & Rozyczka, M. 1998, *Science*, 281, 2025
- Liu, M. C., Najita, J., & Tokunaga, A. T. 2003, *ApJ*, 585, 372
- Loktin, A. V. & Beshenov, G. V. 2001, *Astronomy Letters*, 27, 386
- Lucas, P. W. & Roche, P. F. 2000, *MNRAS*, 314, 858
- Luhman, K. L. 1999, *ApJ*, 525, 466
- Luhman, K. L., Stauffer, J. R., Muench, A. A., et al. 2003, *ApJ*, 593, 1093
- Magnier, E. A. & Cuillandre, J.-C. 2004, *PASP*, 116, 449
- Martín, E. L., Zapatero Osorio, M. R., & Rebolo, R. 1998, in *ASP Conf. Ser. 134: "Brown Dwarfs and Extrasolar Planets"*, eds. R. Rebolo, E. L. Martín, and M. R. Zapatero Osorio, p 507
- Melotte, P. J. 1915, *Mem. R. Astron. Soc.*, 60, 175
- Moraux, E., Bouvier, J., Stauffer, J. R., & Cuillandre, J.-C. 2003, *A&A*, 400, 891
- Muench, A. A., Lada, E. A., Lada, C. J., & Alves, J. 2002, *ApJ*, 573, 366
- Natta, A., Testi, L., Comerón, F., et al. 2002, *A&A*, 393, 597
- Oliveira, J. M., Jeffries, R. D., Devey, C. R., et al. 2003, *MNRAS*, 342, 651
- Oliveira, J. M., Jeffries, R. D., Kenyon, M. J., Thompson, S. A., & Naylor, T. 2002, *A&A*, 382, L22
- Padoan, P. & Nordlund, Å. 2002, *ApJ*, 576, 870
- Papaloizou, J. C. B. & Terquem, C. 2001, *MNRAS*, 325, 221
- Perryman, M. A. C., Lindegren, L., Kovalevsky, J., et al. 1997, *A&A*, 323, L49
- Pinfield, D. J., Hodgkin, S. T., Jameson, R. F., et al. 2000, *MNRAS*, 313, 347
- Röser, S. & Bastian, U. 1994, *A&A*, 285, 875
- Rebolo, R., Martín, E. L., Basri, G., Marcy, G. W., & Zapatero-Osorio, M. R. 1996, *ApJL*, 469, L53
- Rebolo, R., Martín, E. L., & Magazzù, A. 1992, *ApJL*, 389, L83
- Rebolo, R., Zapatero-Osorio, M. R., & Martín, E. L. 1995, *Nat*, 377, 129
- Reid, I. N., Gizis, J. E., Kirkpatrick, J. D., & Koerner, D. W. 2001, *AJ*, 121, 489
- Reid, I. N., Kirkpatrick, J. D., Liebert, J., et al. 1999, *ApJ*, 521, 613
- Reipurth, B. & Clarke, C. 2001, *AJ*, 122, 432
- Rieke, G. H. & Lebofsky, M. J. 1985, *ApJ*, 288, 618
- Rucinski, S. M. 1980, *Acta Astronomica*, 30, 373
- . 1987, *PASP*, 99, 487
- Stauffer, J. R., Barrado y Navascués, D., Bouvier, J., Lodieu, N., & McCaughrean, M. 2003, in *IAU Symposium 211, "Brown dwarfs"*, ed. E. L. Martín (San Francisco: ASP), p 163–170
- Stauffer, J. R., Barrado y Navascués, D., Bouvier, J., Morrison, et al. 1999, *ApJ*, 527, 219
- Sterzik, M. F. & Durisen, R. H. 2003, *A&A*, 400, 1031
- Tej, A., Sahu, K. C., C. T., & Ashok, N. M. 2002, *ApJ*, 578, 523
- Testi, L., Natta, A., Oliva, E., et al. 2002, *ApJL*, 571, L155
- Van't-Veer, F. 1980, *Acta Astronomica*, 30, 381
- Watkins, S. J., Bhattal, A. S., Boffin, H. M. J., Francis, N., & Whitworth, A. P. 1998a, *MNRAS*, 300, 1205
- . 1998b, *MNRAS*, 300, 1214
- Whitworth, A. P. & Zinnecker, H. 2004, *A&A*, 427, 299
- Wielen, R. 1971, *A&A*, 13, 309
- Wilking, B. A., Greene, T. P., & Meyer, M. R. 1999, *AJ*, 117, 469
- Zacharias, N., Urban, S. E., Zacharias, M. I., et al. 2004, *AJ*, 127, 3043
- Zapatero Osorio, M. R., Béjar, V. J. S., Martín, E. L., et al. 2000, *Science*, 290, 103
- Zapatero Osorio, M. R., Martín, E. L., & Rebolo, R. 1997, *A&A*, 323, 105